0023-6837/01/8110-1439$03.00/0
LABORATORY INVESTIGATION
Vol. 81, No. 10, p. 1439, 2001

Pancreas Microenvironment Promotes VEGF Expression and Tumor Growth: Novel Window Models for Pancreatic Tumor Angiogenesis and Microcirculation

Yoshikazu Tsuzuki, Carla Mouta Carreira, Maximilian Bockhorn, Lei Xu, Rakesh K. Jain, and Dai Fukumura

Edwin L. Steele Laboratory, Department of Radiation Oncology, Massachusetts General Hospital and Harvard Medical School, Boston, Massachusetts

SUMMARY: Pancreatic cancer has a poor prognosis, and treatment strategies based on preclinical research have not succeeded in significantly extending patient survival. This failure likely stems from the general lack of information on pancreatic tumor physiology, attributable to the difficulties in developing relevant, orthotopic models that accurately reflect pancreatic cancer in the clinic. To overcome this limitation, we developed abdominal wall windows suitable for intravital microscopy that allowed us to monitor angiogenesis and microvascular function noninvasively during tumor growth in vivo. We used two complementary tumor models in mice: orthotopic (human ductal pancreatic adenocarcinoma, PANC-1, grown in the pancreas), and ectopic (PANC-1 grown in the abdominal wall). We found that orthotopic PANC-1 tumors grew faster than the ectopic tumors and exhibited metastatic spread in the late stage similar to advanced pancreatic cancer in the clinic. Orthotopic PANC-1 tumors expressed vascular endothelial growth factor $(VEGF)_{121}$ and $VEGF_{165}$, contained higher levels of tumor cell–derived VEGF protein, and maintained vascular density and hyperpermeability during exponential tumor growth. Orthotopic PANC-1 tumors showed lower leukocyte–endothelial interactions in the early stage of growth. In addition, both $VEGF_{121}$ and $VEGF_{165}$ promoted the growth of PANC-1 cells in vitro. Finally, Anti-VEGF neutralizing antibody inhibited angiogenesis and tumor growth of PANC-1 tumors in both sites. We conclude that the orthotopic pancreas microenvironment enhances VEGF expression, which stimulates growth of PANC-1 tumors (compared with ectopic tumors). The mechanism is autocrine and/or paracrine and also is involved in the maintenance of blood vessels. This comparative system of orthotopic and ectopic pancreatic cancer will provide the rigorous understanding of pancreatic tumor pathophysiology needed for development of novel therapeutic strategies. (*Lab Invest 2001, 81:1439–1451*).

Pancreatic cancer is the fifth leading cause of cancer death in the United States–the five-year survival rate is 4% (Parker et al, 1997) despite extensive surgery and chemotherapy (Hawes et al, 2000). The microenvironment of the pancreas and the unique characteristics of tumors that derive from it presumably contribute to their resistance to treatments. Most pancreatic cancer preclinical studies in animals are conducted with ectopic models (ie, tumors grown in subcutaneous space instead of the pancreas). Although ectopic sites are more easily accessed and studied, there is accumulating evidence that tumors have distinct patterns of gene expression and significantly different physiologic characteristics depending on the site of tumor growth (Fidler, 1991; Fukumura et al, 1997; Hobbs et al, 1998; Kitadai et al, 1995; Pluen et al, 2001). In addition, a transgenic mouse model for beta cell carcinoma has been extensively studied (Hanahan, 1985), and several orthotopic exocrine pancreatic tumor models have also been reported (An et al, 1996; Bruns et al, 1999; Egami et al, 1991). However, few studies have compared growth- and tumor-associated antigens between different sites of tumor implantation (Egami et al, 1991) and systematically analyzed the pathophysiologic characteristics of pancreatic tumors. Angiogenesis is a prerequisite for tumor growth and metastasis (Carmeliet and Jain, 2000; Folkman, 2000), and physiologic functions of tumor vessels are important to understand the delivery and efficacy of therapeutic agents (Jain, 1998). Several studies have examined the microcirculation of exocrine pancreas (Brunicardi et al, 1996; Wayland, 1997), Islet of Langerhans (Brunicardi et al, 1996; McCuskey, 1997), and pancreatic tumors (Schmidt et al, 1999). However, little is known about the functional properties of the vasculature of pancreatic tumors, especially during their progression. Therefore, studies that evaluate angiogenesis are powerful tools for un-

Received June 25, 2001.
YT and CMC contributed equally to this study. This work was supported by National Cancer Institute Grant PO1-CA90124, a Stewart Trust grant, and a Uehara Memorial Foundation grant.
Address reprint requests to: Dr. Dai Fukumura, Department of Radiation Oncology, Massachusetts General Hospital, 100 Blossom Street, COX-7, Boston, MA 02114. E-mail: dai@steele.mgh.harvard.edu

derstanding pancreatic cancer as well as for treatment design.

Vascular endothelial growth factor (VEGF), a multifunctional cytokine, is one of the most powerful regulators of tumor vasculature. It not only promotes angiogenesis by inducing proliferation, migration, and survival of endothelial cells (Ferrara, 1999), but also increases vessel permeability (Dvorak et al, 1999) and leukocyte adhesion (Melder et al, 1996). VEGF is overexpressed in pancreatic tumors (Terris et al, 1998), correlates with local disease progression (Itakura et al, 1997), and may be useful as a prognostic marker for pancreatic cancer (Ellis et al, 1998; Fujimoto et al, 1998). Alternative splicing of a single VEGF gene transcript allows for at least five VEGF protein isoforms of 121, 145, 165, 189, and 206 amino acids in humans (Houck et al, 1991, 1992; Poltorak et al, 1997; Tischer et al, 1991). Different VEGF isoforms may have distinct functional properties in vivo (Carmeliet et al, 1999). Thus, alternative splicing of VEGF is an important mechanism of control of VEGF activities. Nevertheless, little is known about the factors that dictate which isoforms of VEGF are formed in pancreatic cancer and what their specific roles are. The expression of receptors for VEGF was also reported (Itakura et al, 2000; Von Marschall et al, 2000), suggesting that VEGF promotes pancreatic cancer cell growth via autocrine and paracrine mechanisms.

The objectives of this study were (1) to establish an experimental model to monitor physiologic parameters in normal pancreas and pancreatic tumors, (2) to characterize growth kinetics and pathology of human PANC-1 tumors grown within orthotopic and ectopic environments, (3) to systematically evaluate differences in vascular functions in these tumors during growth by intravital fluorescence microscopy, (4) to determine whether orthotopic and ectopic tumors express different VEGF splice variants, (5) to quantify host- and tumor cell–derived VEGF protein levels in PANC-1 tumors, (6) to determine whether VEGF isoforms differentially promote tumor cell growth in vitro, and (7) to determine the effect of Anti-VEGF antibody treatment on angiogenesis and tumor growth in orthotopic and ectopic PANC-1 tumors. These new models, as well as the novel findings of the role of VEGF in pancreatic cancer pathophysiology, should provide useful information for the design of cancer treatments.

Results

Faster Tumor Growth and Higher Incidence of Invasion and Metastasis in Orthotopic PANC-1 Tumors

After surgical implantation in severe combined immunodeficient (SCID) mice, PANC-1 cells formed growing solid tumor masses in both orthotopic (pancreas) and ectopic (abdominal wall) sites. Tumor take rate was more than 95% at both sites. Both orthotopic and ectopic tumors had a white to translucent appearance with some macroscopically identifiable blood vessels and thus were clearly distinguishable from surrounding normal pancreas or abdominal wall tissue (Fig. 1). The growth rate of PANC-1 tumors is shown in Figure 2. In the early stage, there was no significant difference in tumor growth between orthotopic and ectopic sites. Five weeks after tumor implantation, orthotopic tumors started growing significantly faster than in an earlier period. Ectopic tumors started to grow faster 6 weeks after tumor implantation. Orthotopic PANC-1 tumors were significantly larger than the ectopic tumors 5 weeks after tumor implantation and remained so until the end of the experiments (8 weeks). In the late stage, orthotopic PANC-1 tumors showed macroscopic invasion of peritoneum, mesentery, spleen, kidney, and retroperitoneum. Frequent metastases to the mesenteric lymph nodes and a few metastatic foci in the liver were also present. Distant metastases in the brain or lung were not found macroscopically. In contrast, ectopic tumors showed neither direct invasion into the peritoneal cavity nor any distal metastases.

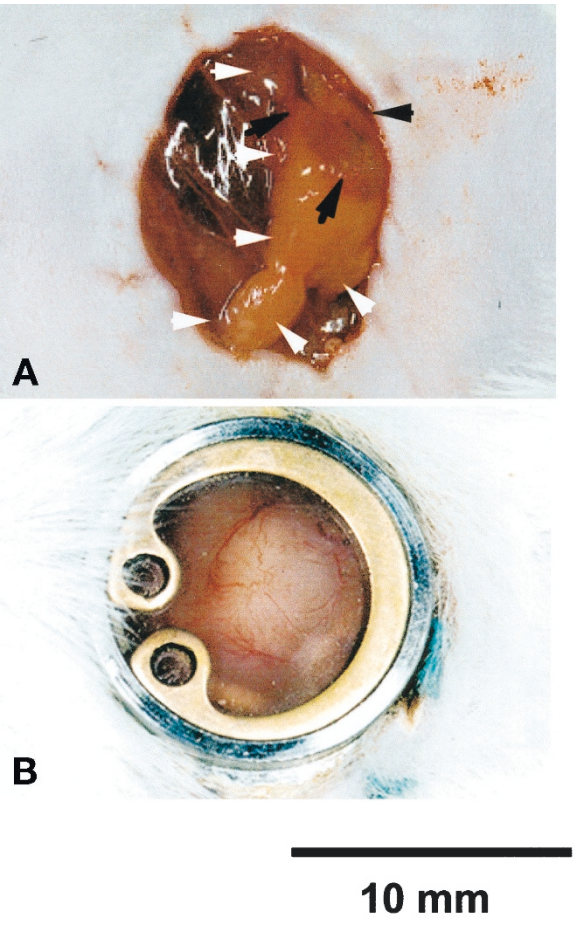

Figure 1.
Human ductal pancreatic adenocarcinoma (PANC-1) tumor grown in pancreas and abdominal wall window preparation. A, Exteriorized pancreas and orthotopic PANC-1 tumor. Four weeks after the tumor implantation on the splenic lobe of pancreas, tumor in the pancreas was exteriorized through an incision in the abdominal wall. A white to translucent tumor (*black arrow*), 5–6 mm in diameter, was seen in the pancreas (*white arrows*), which is pinkish. B, Orthotopic PANC-1 tumor in the abdominal wall window. Orthotopic tumor (white) with blood vessels is shown.

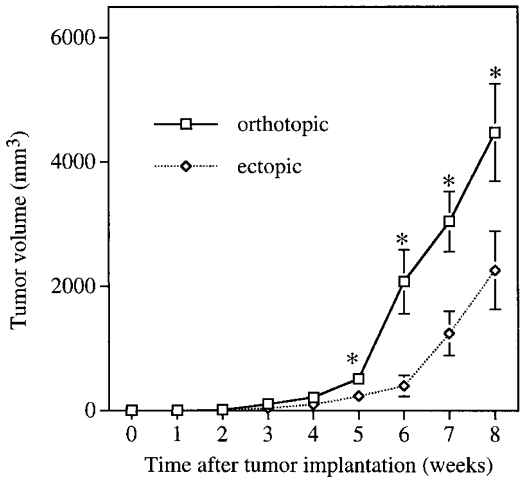

Figure 2.
Growth of orthotopic and ectopic PANC-1 tumors. Tumor size was measured by a caliper after laparotomy or skin incision weekly in both orthotopic and ectopic sites. Five weeks after tumor implantation and later, the orthotopic tumors were significantly larger than the ectopic tumors. These measurements were made in at least five animals per group at each time point. $^*p < 0.05$ compared with corresponding ectopic tumor.

Orthotopic PANC-1 Tumors Mimic Histologic Features of Advanced Pancreatic Cancer

Hematoxylin and eosin staining revealed that orthotopic PANC-1 tumors were poorly differentiated invasive adenocarcinomas. As shown in Figure 3, there was no gland-like structure, and extensive tumor cell invasion into the host pancreas was observed at the tumor-host interface. As a result of invasion and growth of the tumor, normal pancreas tissue islands surrounded by tumor cells were frequently found. It is noteworthy that significant tissue reaction was present in the periphery of the orthotopic PANC-1 tumors. Adjacent to the tumor, large reactive fibromatous tissue with infiltrating fibroblasts, macrophages, granulocytes, and monocytes was often observed. On the other hand, ectopic PANC-1 tumors showed large central necrosis and many apoptotic cells. At the tumor periphery, invasion into the host muscle cell layer and tissue reaction were both observed to some extent.

Disorganized Blood Vessel Architecture in PANC-1 Tumors

Newly developed abdominal windows were implanted into control mice (for normal pancreas) and orthotopic and ectopic tumor-bearing mice at 4 weeks after tumor implantation (Fig. 1B). Fluorescein isothiocyanate (FITC)-dextran, injected systemically, was used to visualize blood vessels under epi-illumination (Fig. 4). In the normal pancreas, a regular vascular architecture was observed. Arterioles were straight, rela-

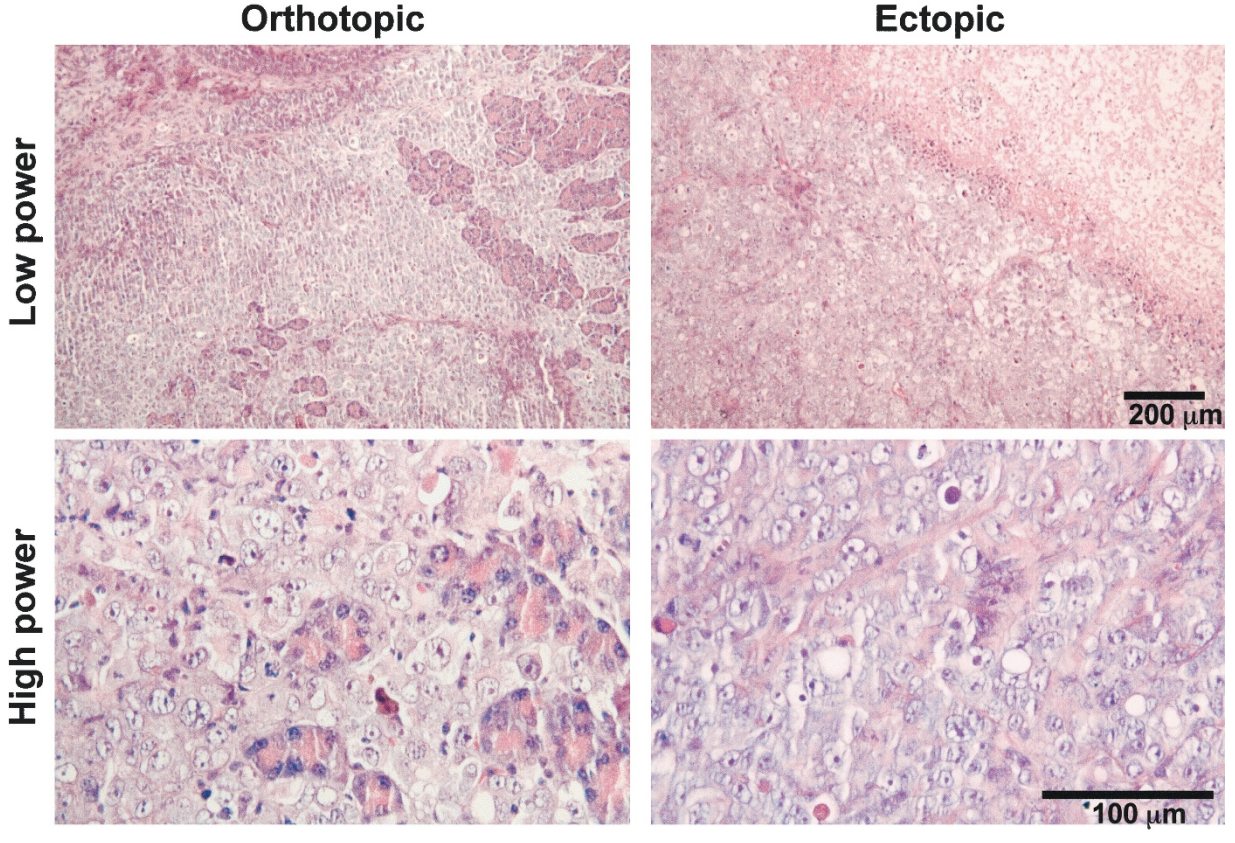

Figure 3.
Hematoxylin-eosin staining of orthotopic and ectopic PANC-1 tumor. *Left column*, Low and high magnification views of orthotopic tumors demonstrate poorly differentiated invasive adenocarcinoma. Massive tumor cell invasion into the host pancreas and normal pancreas glands surrounded by tumor cells are observed. *Right column*, Low and high magnification views of ectopic tumor showed extensive central necrosis and many apoptotic cells.

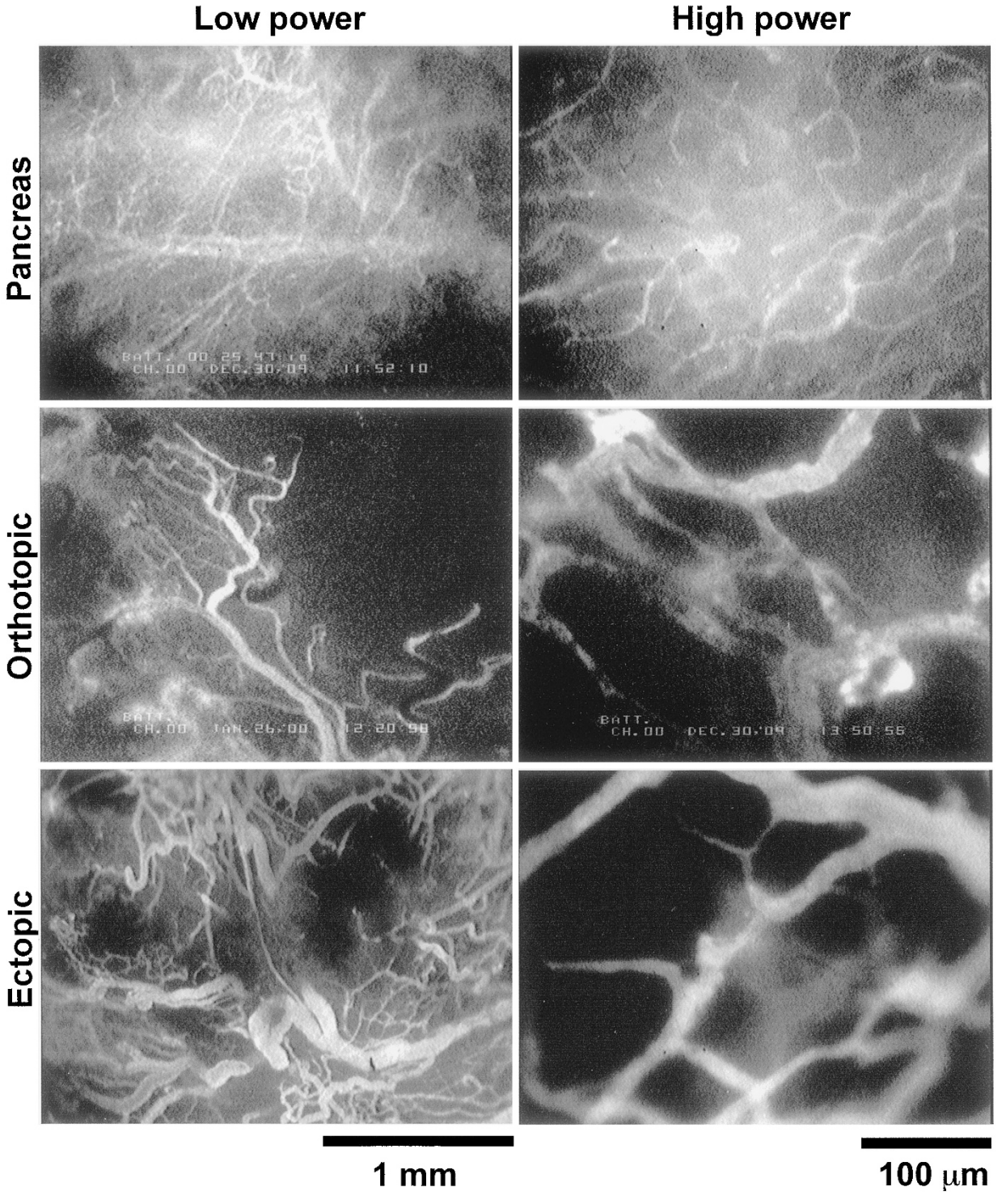

Figure 4.
Microscopic images of normal pancreas and PANC-1 tumors. FITC-labeled dextran solution was injected into mouse tail veins for contrast enhancement. Using FITC fluorescence images, blood vessels in pancreas and PANC-1 tumors were visualized. *Upper row*, Vasculature of normal pancreas. Arterioles were straight and relatively small in diameter and branched into capillaries (left). An organized and high-density capillary network was observed in high magnification image (right). *Middle row*, Vasculature in orthotopic PANC-1 tumor. In the tumor, blood vessels are larger and tortuous. Vessel density is lower compared with normal pancreas. The distribution of blood vessels was heterogeneous. Note the avascular region in the low magnification image (left). *Lower row*, Vasculature in ectopic PANC-1 tumor. Overall, vessel architecture was similar to that in the orthotopic tumor.

tively small in diameter, had high flow rates (compared with venules), and eventually branched into capillaries. Capillaries (approximately 9 μm in diameter) formed a high-density vascular network, which then collected into postcapillary venules. In contrast, tumor vasculature was irregular and tortuous. Tumor vessels were

often larger in diameter, of lesser density, and had an irregular wall shape and branching pattern. Blood flow was sluggish and sometimes static. Furthermore, distributions of blood vessels and flow in the tumor were spatially and temporally heterogeneous. Some regions were completely avascular, whereas adjacent regions were relatively well vascularized. There was no significant morphologic difference in blood vessels between orthotopic and ectopic PANC-1 tumors. Overall, PANC-1 tumors showed chaotic and disorganized blood vessels, in agreement with previous findings in other tumors (Fukumura et al, 1997; Jain, 1997; Leunig et al, 1992).

Stable Vascular Density in Orthotopic PANC-1 Tumors

We determined linear vascular density as a functional parameter of angiogenesis. Linear vascular density (cm/cm^2) is the total length of functional blood vessels in a given area. This parameter is inversely proportional to the average diffusion distance between the blood vessels and the cells. As shown in Table 1, vessel density was significantly lower in PANC-1 tumors compared with normal pancreas, regardless of site or size. Vessel density in the ectopic tumors decreased significantly during tumor growth. On the other hand, vessel density in the orthotopic tumor tended to increase during exponential tumor growth. As a result, vessel density in the orthotopic tumors was significantly higher than that in the ectopic tumors.

Stable Blood Flow in Orthotopic PANC-1 Tumors

Although blood flow in both orthotopic and ectopic tumors was often sluggish and heterogeneous, overall red blood cell (RBC) velocity in individual functioning vessels was comparable among the various tumors, regardless of size or growth site (Table 1). Initially, ectopic PANC-1 tumor vessels had higher blood flow rates due to the larger vessel diameters. After further tumor growth, the flow rate in the ectopic implantations decreased. In contrast, average flow rate in the orthotopic tumor vessels was stable over 8 weeks of tumor growth.

High Vascular Permeability in PANC-1 Tumors

Vascular permeability in PANC-1 tumors was one order of magnitude higher than that in normal vessels (Table 1). However, there was no statistical difference in vascular permeability between different tumor sites or sizes.

Lower Leukocyte Adhesion in Early Stage of Orthotopic PANC-1 Tumors

In our pancreatic tumor models, we found that both leukocyte rolling and adhesion were significantly lower in the orthotopic tumors than in the ectopic tumors at the early stages. However, leukocyte adhesion was significantly increased when the orthotopic tumors grew further (Table 1). Despite the change in the number of adherent leukocytes along the vessel during tumor growth, total leukocyte flux into the vessels in the orthotopic PANC-1 tumors remained significantly lower than that in the ectopic tumors. In the vessels examined for leukocyte endothelial interactions, wall shear rates were comparable among the various tumor sites and sizes.

The Same Splice Variants of VEGF Were Detectable in Orthotopic and Ectopic PANC-1 Tumors

Using RT-PCR with primers specific to different exons within the human and mouse VEGF-A genes (Fig. 5A), we found that the same VEGF-A transcripts ($VEGF_{120/121}$ and $VEGF_{164/165}$) were expressed in both orthotopic and

Table 1. Physiologic Parameters in PANC-1 Tumors

	Early stage (4 wk)		Late stage (8 wk)		Normal pancreas
	Orthotopic	Ectopic	Orthotopic	Ectopic	
Angiogenesis					
Vascular density (cm/cm^2)	100 ± 14	122 ± 12	124 ± 17*	77 ± 10#	254 ± 6
Vessel diameter (μm)	20 ± 1	22 ± 1	15 ± 1*#	20 ± 1	9.1 ± 0.4
Permeability					
Vascular permeability ($\times 10^{-7}$ cm/s)	3.1 ± 1.0	4.9 ± 1.1	3.1 ± 1.0	4.6 ± 0.8	0.5 ± 0.1
L/E interaction					
Rolling rate (%)	31 ± 2*	45 ± 2	39 ± 4	35 ± 3	
Adhesion ($cells/mm^2$)	48 ± 7*	93 ± 13	130 ± 28#	186 ± 50	
Total flux (cells/30 s)	13 ± 2*	22 ± 3	16 ± 1*	26 ± 4	
Shear rate (l/s)	29 ± 6	17 ± 4	27 ± 5	16 ± 2	
Hemodynamics					
RBC velocity (mm/s)	153 ± 3	159 ± 4	161 ± 6	161 ± 8	169 ± 2
Blood flow (pl/s)	40 ± 5	84 ± 9*	32 ± 4	43 ± 5#	9 ± 1

PANC, pancreatic adenocarcinoma; L/E, leukocyte-endothelial; RBC, red blood cell.
N = 3–12 for each group.
* $p < 0.05$ compared with ectopic PANC-1 tumor; # $p < 0.05$ compared with early stage tumor.

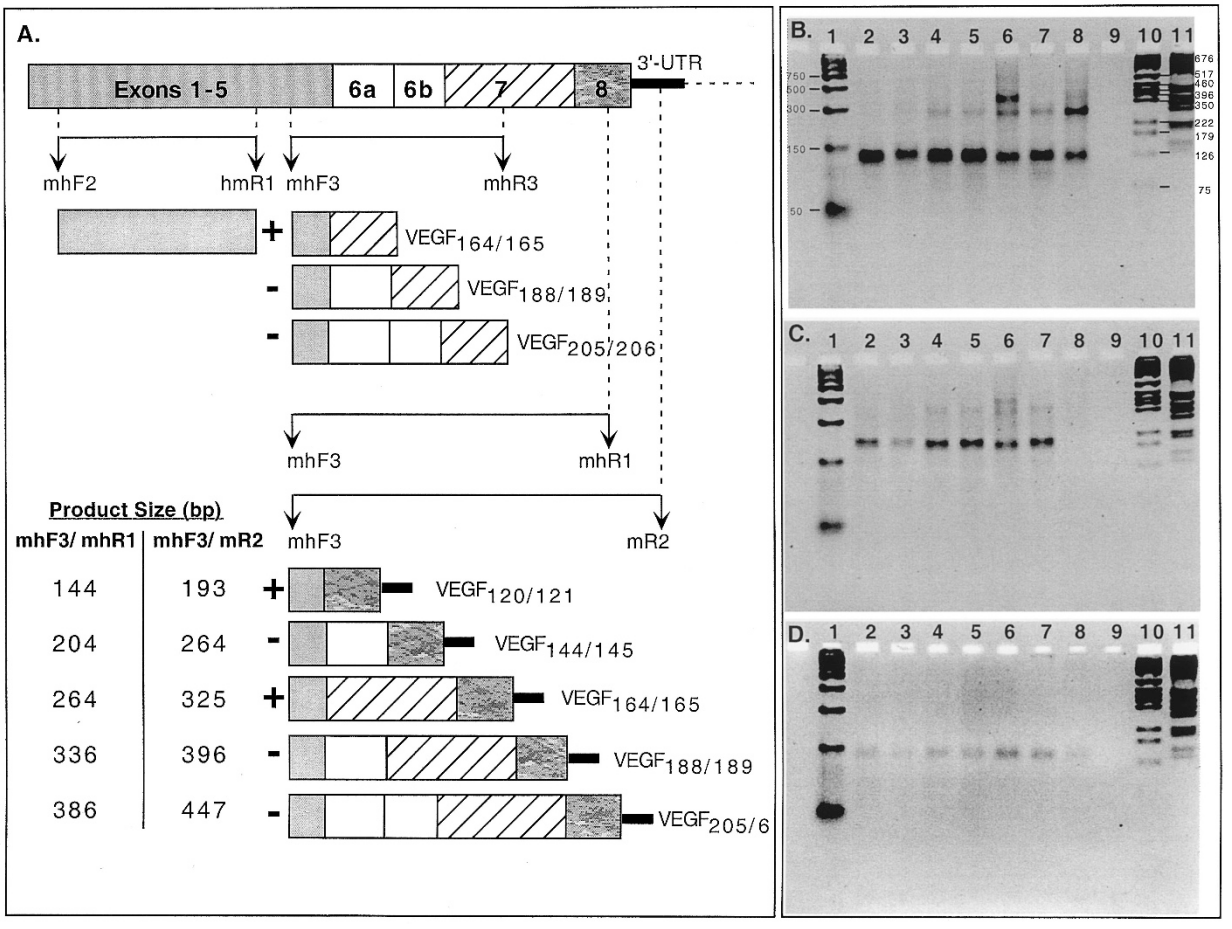

Figure 5.

Vascular endothelial growth factor (VEGF)-A 120/121 and 164/165 splice variants expressed in orthotopic and ectopic PANC-1 tumors. Primer sets were designed to allow discrimination of the alternative VEGF-A splice variants on the basis of the size of the products obtained by RT-PCR (A). The approximate position of the sequences with which they hybridize is represented by the *vertical arrows*. PCR reactions were performed with primer sets VEGFmhF3/mhR1 (B), VEGFmhF3/mR2 (C), and HPRTmhF1/mhR1 (D) using no cDNA (Lane 9) or cDNA prepared from PANC-1 tumors (Lanes 2 through 5: early orthotopic, late orthotopic, early abdominal wall, late abdominal wall, respectively) or normal tissues (Lane 6: mouse lung; Lane 7: mouse ovary; Lane 8: human brain). The plus (+) or minus (−) sign on the left of each diagram indicates detectable or nondetectable specific splice variants, respectively. Primer sets mhF2/hmR1 (from a region conserved among all VEGF-A variants) and mhF3/mhR3 (to discriminate between exon 7–containing variants) were also used as further controls (data not shown). Product sizes were compared with known markers: PCR marker (Lane 1), pGEM (Lane 10), and 1kb ladder (Lane 11). The drawing is not to scale.

ectopic PANC-1 tumors (Fig. 5, B and C, Lanes 1 through 4). In addition, we were able to detect one additional transcript of VEGF-A in the mouse lung and human brain tissues (Fig. 5B, Lanes 6 and 8, respectively) and its size is in agreement with what we predicted for $VEGF_{206}$ (Fig. 5A). Furthermore, because the primer mR2 recognizes mouse but not human VEGF sequence (Fig. 5C, Lanes 6 and 7 vs Lane 8), at least some of the $VEGF_{120/121}$ and $VEGF_{164/165}$ transcripts we detected in these tumors were from cells of host (mouse) origin. Finally, the presence of human $VEGF_{164/165}$ (but not $VEGF_{189}$ or $VEGF_{206}$) in these tumors was confirmed with another set of primers (mhF3/mhR3; data not shown). Thus, no qualitative differences in VEGF-A mRNA splicing were observed over time or between tumor sites in our models. Although we could distinguish tumor-derived and host-derived VEGF-A mRNA, the detection of multiple products in the same PCR reaction prevented further quantitative analysis of gene expression in each site from these and quantitative RT-PCR data (not shown).

Higher Human VEGF Protein Level in the Late Stage Orthotopic PANC-1 Tumors

It was first necessary to determine the species specificity of the VEGF detection kits. We confirmed that the human VEGF kit did not detect either recombinant mouse VEGF (100 ng/ml) or VEGF in extracts from mouse embryonic stem (ES) cells (which contain VEGF by other assays) (Carmeliet et al, 1998; Tsuzuki et al, 2000), but was able to detect human recombinant VEGF (20–2,000 pg/ml) and VEGF in cultures of human colon cancer cells LS174T (not shown). Similarly we established that the mouse VEGF kit did not detect human recombinant VEGF (200 ng/ml) or VEGF from human colon adenocarcinoma cells (ATCC, Rockville, Maryland), but detected mouse recombinant VEGF (3–500 pg/ml) and VEGF from mouse ES cells. Next, we measured human- and mouse-derived VEGF in the tumors (Fig. 6). At the early stages of tumor growth, no significant difference was seen in host cell–derived (mouse; Fig. 6B) or cancer cell–derived (human; Fig.

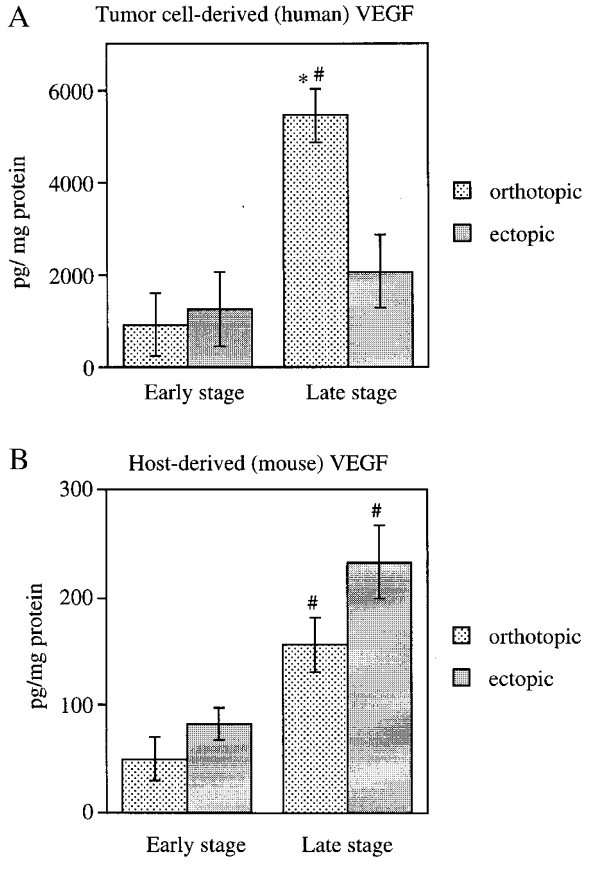

Figure 6.
ELISA for VEGF protein expression in orthotopic and ectopic PANC-1 tumors. Tumor-derived human VEGF and host-derived mouse VEGF were determined by ELISA specific to human and mouse VEGF, respectively. A, Tumor-derived human VEGF. VEGF level was higher in the late stage (8 weeks after tumor implantation) than in the early stage (4 weeks after tumor implantation). In the late stage, the orthotopic tumors exhibited higher VEGF levels than the ectopic tumors. B, Host-derived mouse VEGF. Host stromal cell–derived VEGF also increased with tumor growth. However, the magnitude of host-derived VEGF was one order of magnitude lower than tumor-derived VEGF. $n = 3$ for each group. $*p < 0.05$ compared with corresponding ectopic tumor. $\#p < 0.05$ compared with corresponding early stage tumor.

6A) VEGF between implantation sites. However, in late-stage tumors (8 weeks), orthotopic PANC-1 tumors had significantly higher levels of cancer cell–derived VEGF than the ectopic tumors (Fig. 6A); such a difference was not noted in host-derived VEGF. In addition, although both cancer cell–derived (human) and host cell–derived (mouse) VEGF levels seemed to increase over time, this increase was only statistically significant in orthotopic tumors. Finally, the relative contribution of cancer cells to the production of VEGF protein was significantly higher than the contribution of the host in these models.

Both $VEGF_{121}$ and $VEGF_{165}$ Induce PANC-1 Cell Proliferation

3-(4, 5-dimethythiazol-2-yl)-2,5-diphenyl-tetrazolium bromide (MTT) assays showed that both $VEGF_{121}$ and $VEGF_{165}$ at 5 ng/ml significantly increased PANC-1 cell proliferation under serum deprivation and these effects were reversed with the administration of anti-human VEGF neutralizing antibody (Fig. 7). Cell proliferation induced by each VEGF isoform (in the absence of serum) was significantly higher than in serum-free culture (with no VEGF added) at 48 hours of incubation. Both human VEGF isoforms ($VEGF_{121}$ and $VEGF_{165}$) and murine VEGF isoforms ($VEGF_{120}$ and $VEGF_{164}$) showed similar effects on PANC-1 cell proliferation at 1 ng/ml and 10 ng/ml (not shown). Addition of Anti-VEGF neutralizing antibody consistently abrogated the effect of VEGF.

Anti-VEGF Neutralizing Antibody Inhibits Angiogenesis and Tumor Growth

To ascertain the role of VEGF in modulating the pathophysiologic characteristics of orthotopic and ectopic tumors, we treated PANC-1 tumors grown in different sites with Anti-VEGF neutralizing antibody. We started the treatment at 4 weeks after tumor implantation and continued the treatment for 4 weeks. As shown in Figure 8, Anti-VEGF antibody (Ab) treatment significantly reduced vascular density in the orthotopic tumors. Furthermore, Anti-VEGF Ab–treated tumors in the orthotopic and ectopic sites had comparable vessel densities. Vessel diameter in the ectopic tumors was significantly smaller in Anti-VEGF Ab–treated group than in the control Ab–treated group. Under the control Ab treatment, both orthotopic and ectopic tumors grew significantly in 4 weeks (Fig. 9). However, the tumors did not grow significantly during Anti-VEGF Ab treatment regardless of the growth site.

Discussion

We have established a novel system for pancreatic cancer studies that allowed us to monitor and compare tumor growth and its physiologic parameters in ortho-

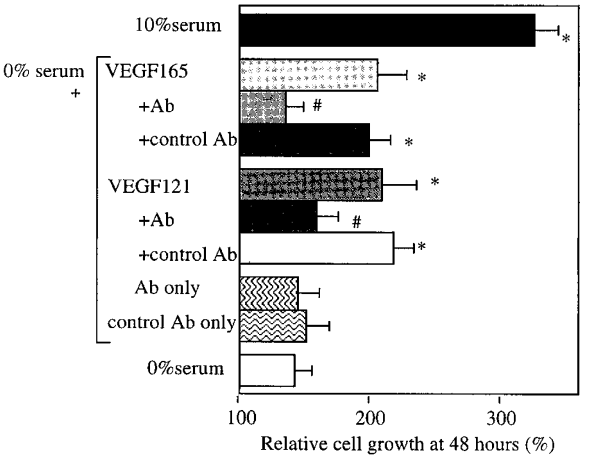

Figure 7.
Effect of VEGF isoforms on PANC-1 cell proliferation. The effect of VEGF on tumor cell proliferation was assessed by 3-(4, 5-dimethythiazol-2-yl)-2,5-diphenyl-tetrazolium bromide (MTT) dye reduction assay. Relative changes of optical density to the corresponding baseline values are presented. $*p < 0.05$ compared with 0% serum. $\#p < 0.05$ compared with corresponding VEGF administration.

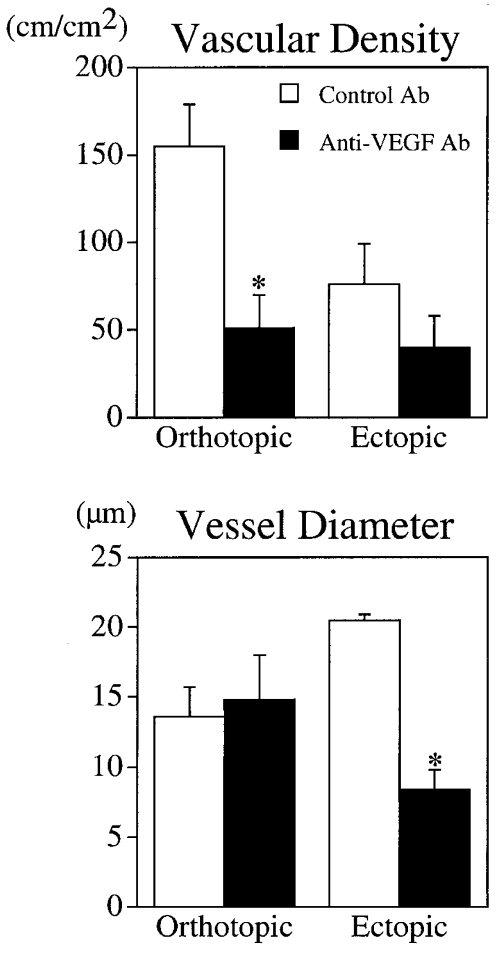

Figure 8.
Effect of Anti-VEGF antibody (Ab) on angiogenesis in PANC-1 tumors. PANC-1 tumors were treated with Anti-VEGF Ab or control Ab for 4 weeks. Vascular density and diameter were determined by intravital microscopy. $*p < 0.05$ compared with corresponding control Ab-treated group.

topic and ectopic environments. We found that PANC-1 tumors grow more favorably within the pancreas (orthotopic site) than on the exterior surface of the abdominal wall (ectopic site), consistent with previous reports that orthotopic tumor xenografts grow faster than tumors implanted in ectopic sites such as subcutaneous spaces (Egami et al, 1991; Fidler, 1991). In patients, pancreatic adenocarcinoma spreads via direct invasion into the retroperitoneal area or adjacent organs, or by peritoneal dissemination and metastases to mesenteric lymph nodes and the liver in the advanced stage (Ellenrieder et al, 1999; Hawes et al, 2000). Indeed, in the late stages (8 weeks after implantation), orthotopic PANC-1 tumors showed these same clinical features. In addition, our orthotopic tumors spread less often by lymphatic metastasis than by blood-borne metastasis to the liver. These features are also consistent with pancreatic cancer in the patients. On the other hand, the ectopic tumors showed less invasion and virtually no metastases. It is the invasive, highly metastatic primary tumors that are likely to kill patients; our orthotopic model has these characteristics and is likely to affect our understanding of patients' response to treatments (Fidler et al, 1994).

VEGF is one of the most potent angiogenic factors overexpressed in various solid tumors, including pancreatic cancer (Ferrara, 1999). In this study, we found that VEGF protein levels increased with tumor growth in both orthotopic and ectopic PANC-1 tumors. More importantly, VEGF in late-stage orthotopic tumors was significantly elevated (5-fold higher than the early stage tumors and 3-fold higher than the ectopic tumors in the late stage). We also found that the orthotopic tumors exhibited stable vascular density and blood flow during growth, whereas the ectopic tumors lost significant levels of both vascular density and blood flow during the exponential growth phase. Actual tumor growth rate increased in the later stages; therefore, angiogenesis had to accelerate to maintain a constant vascular density. This suggests that increased VEGF supported active vessel growth and maintained blood supply during exponential tumor growth in the orthotopic tumors. On the other hand, the VEGF levels may not be high enough to maintain vessels and blood supply in the ectopic tumors, resulting in central necrosis. Differences in vascular densities between sites could be due to variability in the local levels of angiostatic factors such as endostatin and transforming growth factor (TGF)-β1 (Gohongi et al, 1999), organ-specific characteristics of tissue extracellular matrices, and other angiogenic factors such as fibroblast growth factor. Interestingly, total tissue VEGF protein levels in PANC-1 tumors were 1–6 ng/mg protein. These values are 2- to 10-fold higher than those in subcutaneously growing sarcomas or ES cell–derived teratomas (Tsuzuki et al, 2000). However, vascular densities in PANC-1 tumors were comparable or even lower than in these tumors (60–150 cm/cm^2). These results again suggest that pancreatic tumors produce endogenous antiangiogenic factors. Alternatively, the angiogenic response of the endothelium to VEGF may be host organ–dependent. Indeed, endothelial cells have organ-specific phenotypes and specialized properties (Carmeliet and Jain, 2000; Ruoslahti and Rajotte, 2000). Finally, the metabolic organ microenvironment and its interaction with neoplastic cells may modulate the VEGF response in vivo.

The permeability of PANC-1 tumor vasculature at both sites was significantly higher than in normal pancreas. However, we were surprised to observe no significant differences in vascular permeability between tumor sites or in various stages of growth, especially since the orthotopic tumors had higher VEGF protein levels. One possible interpretation is that vascular permeability might reach an organ-dependent plateau at a certain VEGF level (Jain and Munn, 2000; Monsky et al, 1999; Tsuzuki et al, 2000). Furthermore, differential expression of other regulators of vessel permeability, such as the Angiopoietins-Tie system, may be involved (Jain and Munn, 2000).

Through the use of reagents that make total mouse and human VEGF distinguishable (ie, independently of its isoforms), we found that PANC-1 tumor cells are the major contributor to VEGF production in our pancreatic tumor models. However, it is noteworthy that

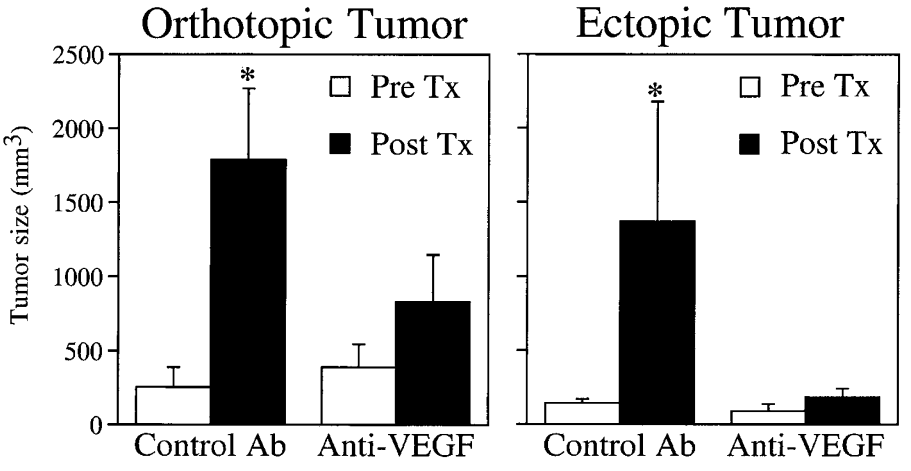

Figure 9.
Effect of Anti-VEGF Ab on PANC-1 tumor growth. From 4 (*Pre Tx*) to 8 (*Post Tx*) weeks after the implantation, PANC-1 tumors treated with Anti-VEGF Ab or control Ab. $*p < 0.05$ compared with corresponding pretreatment value.

the amount of VEGF produced by host stromal cells in pancreatic tumors is comparable to VEGF production by host stromal cells in subcutaneously growing teratomas (Tsuzuki et al, 2000). Whereas VEGF production from nonneoplastic cells is determined by microenvironmental characteristics, such as tissue oxygen level, pH, and cytokines, neoplastic cells have additional induction mechanisms through oncogene activation (Izuishi et al, 2000) or other gene mutations. Thus, advanced stage pancreatic tumors express large amounts of VEGF, which can lead to increased angiogenesis, invasion, metastasis, and poor prognosis (Dvorak et al, 1999; Ferrara, 1999).

In normal tissue, the expression of VEGF receptors such as flt-1 and flk-1 is thought to be vascular endothelial cell–specific (Ferrara, 1999). However, some tumor cells do express these receptors, including the PANC-1 cell line, which expresses Flt-1 (Itakura et al, 2000; Von Marschall et al, 2000). Here, we showed that both $VEGF_{121}$ and $VEGF_{165}$ induced PANC-1 cell proliferation in vitro and this effect was reversed by antihuman VEGF antibody. Thus, in addition to promoting the recruitment of blood vessels, at least two VEGF isoforms induce tumor cell proliferation directly and could aggressively promote invasion and metastasis in pancreatic cancer through autocrine/paracrine mechanisms. In addition to VEGF/VEGFR, other autocrine growth-promoting systems, such as EGF-EGFR and TGFβ-TGFR-II that are disregulated in pancreatic cancer cells, may be involved as well (Friess et al, 1995).

The Anti-VEGF neutralizing antibody used in this study is currently in clinical trials for various malignant tumors. In addition, various approaches for blocking VEGF-receptor signaling pathways, such as soluble Flt-1 protein, anti-Flk-1 receptor antibody, and synthetic compounds that inhibit phosphorylation of VEGF receptors, have been extensively investigated in both experimental and clinical settings. Our results not only confirm the role of VEGF in the maintenance of blood vessels and tumor growth of orthotopic PANC-1 tumors, but also strongly support the use of Anti-VEGF strategies for the treatment of patients with pancreatic cancer.

In summary, our orthotopic PANC-1 tumor model presents features of advanced pancreatic cancer in humans. The ability to study the kinetics of tumor growth along with intravital observation of functional vascular density revealed that orthotopic tumors grow faster than ectopic tumors. Presumably this is because of stable vascular density, regardless of the tumor size, and higher VEGF levels that induce angiogenesis and tumor cell proliferation via both direct and indirect mechanisms. Our model for pancreatic cancer allows time-course studies using a novel abdominal wall window and permits careful comparison of tumors in orthotopic and ectopic sites. The result is a more rigorous understanding of the pathophysiology of pancreatic cancer and support for blocking VEGF as a promising new treatment strategy.

Materials and Methods

Cell Line and Tumor Source Preparation

PANC-1 cells were derived from a poorly differentiated human pancreatic ductal adenocarcinoma (Lieber et al, 1975) and were obtained from the American Type Culture Collection (ATCC) (Rockville, Maryland). Cells were grown as adherent cultures in DMEM with 10% FBS in a humidified 5% CO_2 atmosphere. Cells were trypsinized to prepare single-cell suspensions and a centrifuged pellet containing 1×10^6 cells was then injected subcutaneously into SCID mice. Tumors were allowed to grow for 6 to 8 weeks, and then dissected. Small pieces of viable tumor tissue (approximately 1 mm in diameter) were used as tumor source.

Tumor Implantation

Male SCID mice (25–30 g) were used. All animal protocols were approved by the institutional animal care and use committee. The entire procedure was

performed under sterile conditions inside a gnotobiotic animal facility in our department. Mice were anesthetized with Ketamine and Xylazine (90 mg/9 mg per kilogram of body weight). The hair on the left flank was shaved. For orthotopic tumor implantation, a small left lateral laparotomy was performed. The splenic lobe of the pancreas was gently exteriorized from the abdominal cavity. A small piece of PANC-1 tumor was sutured to the serosal side of the pancreas with a 5–0 prolene (Ethicon, Somerville, New Jersey). The abdominal wall and the skin were sutured and closed. For ectopic tumor implantation, the skin of the left flank was cut, a small piece of tumor was sutured directly to the outer side of the abdominal wall, and the overlying skin was closed by a suture.

Measurements of Tumor Growth

Mice bearing orthotopic or ectopic tumors were anesthetized and laparotomy or skin incision was performed, respectively. The size of the tumor was measured by a caliper. Tumor volume was calculated as $\pi/6 \times a \times b \times c$ (where a is longitudinal diameter, b is short diameter, and c is thickness). These measurements were made every week after tumor implantation (in different animals) with at least five animals per group for up to 8 weeks. After the tumor size measurements, the mice were killed for subsequent tissue analysis.

Abdominal Window Preparation

To observe tumor microcirculation, we implanted abdominal wall windows 4 weeks after orthotopic tumor implantation (tumor size approximately 6–8 mm in diameter). The skin and abdominal wall over the pancreas were reopened, the splenic lobe of the pancreas (with a growing tumor) was gently exteriorized, and a portion of normal pancreas was sutured to the outer side of the abdominal wall. A titanium circular mount with 8 holes on the edge (15 mm outer diameter, 11 mm inner diameter, and 1 mm thick, custom-made in our machine shop) was inserted between the skin and abdominal wall. This method holds the pancreas and tumor inside the window. Then a circular glass coverslip (11.7 mm diameter; Fisher Scientific, Pittsburgh, Pennsylvania) was placed on top and fixed by a snap ring. Throughout the procedure, the surface of the tumor and pancreas was kept moist with prewarmed buffered saline solution. In a separate set of experiments, we implanted abdominal wall windows for normal pancreas. We also implanted abdominal wall windows 4 weeks after the ectopic tumor implantation (tumor diameter approximately 6–8 mm) by a procedure similar to the orthotopic model.

After window implantation, tumors were monitored daily and subsequently used for intravital microscopy studies when tumors reached the desired size. For intravital microscopy, mice were anesthetized, the tail vein was cannulated for intravenous injections of fluorescent tracers, and then the mice were placed inside a plastic tube (25 mm inside diameter) with a slit of 14 mm $\times$ 37 mm wide. The abdominal wall window was fitted in the slit of the plastic tube and fixed by Transpore tape (3M, Minneapolis, Minnesota) to minimize the influence of respiratory movements during measurements. Our new abdominal wall window model allowed us to monitor tumors up to 10 mm in diameter. For larger tumors (8 weeks after PANC-1 tumor implantation), we used a specially designed microscope stage to hold tumors under a microscope (Fukumura et al, 1997). New vessel formation, blood flow, and various other physiologic parameters were then assessed by intravital microscopy with epi-illumination.

Intravital Microscopy

Animals bearing tumors and control animals (for studies of normal pancreas) were anesthetized and observed by intravital microscopy at 4 weeks and 8 weeks after tumor implantation. Angiogenesis, hemodynamics, vascular permeability, and leukocyte-endothelial interactions were quantified by intravital microscopy as previously described (Fukumura et al, 1995; Leunig et al, 1992; Yuan et al, 1993). Briefly, to visualize the blood vessels, 100 μl of a 10 mg/ml FITC-labeled dextran solution (MW 2,000,000; Sigma Chemical, St. Louis, Missouri) were injected intravenously. Fluorescence images of five random locations of each tumor or normal pancreas were recorded and digitized for subsequent off-line analysis. Functional vascular density was measured as the total length of perfused vessels per unit area of observation field (NIH Image v.1.6). RBC velocity was measured using temporal correlation velocimetry (Microflow system, model 208C, videophotometer version; IPM, San Diego, California). Vessel diameter was measured with an image-shearing device (digital video image shearing monitor, model 908; IPM). Mean blood flow rates and shear rates of individual vessels were calculated using vessel diameter and mean centerline RBC velocity, as described previously (Leunig et al, 1992). The microvascular permeability to BSA was measured using tetramethylrhodamine-labeled BSA (0.1%, 100 μl; Molecular Probes, Eugene, Oregon), as described previously (Yuan et al, 1993). Leukocyte rolling and adhesion in tumor vessels were measured by monitoring endogenous leukocytes labeled with a bolus (20 μl) of 0.1% rhodamine 6-G (Rho-6G; Molecular Probes) in saline, as described previously (Fukumura et al, 1995).

Histologic Examinations

Tumors grown in orthotopic or ectopic sites were excised, fixed in formalin, and paraffin-embedded. Five-micrometer tissue sections were used for hematoxylin and eosin staining.

RT-PCR for Profiling of VEGF Splice Variants in Tumors

Preparation of RNA. Tumors were excised, immediately frozen in liquid nitrogen, and stored at $-70°$ C until further analysis. Total RNA was isolated from each tumor using RNAzol B (Tel Test B, Friendswood,

Texas) following the manufacturer's protocol. For complete elimination of DNA contamination, each total RNA preparation was subsequently treated with DNaseI using the Message Clean system (GenHunter Corporation, Nashville, Tennessee). RNA obtained by this procedure were typically of high quality as assessed by standard O.D.260/O.D.280 ratio analysis and denaturing gel electrophoresis. RNA were stored in aliquots at −70° C at concentrations higher than 1 μg/μl in DEPC-treated water.

Reverse Transcription. RNA were reverse-transcribed into cDNA using the conditions specified in the TaqMan RT Reagents System (PE Applied Biosystems, Foster City, California). Typically, 1 μg of total RNA from each tumor was reverse-transcribed with oligo $d(T)_{16}$ primers in a final reaction volume of 100 μl.

PCR Amplification. The primers used to detect each splice variant of VEGF-A mRNA (see below and Figure 5) were designed based on (1) the known sequences and exon-intron structures of mouse and human VEGF-A genes (mouse and human isoforms differ by one residue) reported in the GeneBank; (2) their ability to span intron/exon boundaries (to avoid problems from possible DNA contamination); and (3) optimal Tm, minimal hairpin structures, and minimal primer dimer formation. The design was made with the help of Primer 3 software (Steve Rozen, Helen J. Skaletsky, Whitehead Institute for Biomedical Research, 1996, 1997) obtainable as freeware from http://www-genome.wi.mit.edu/cgi-bin/primer/primer3.cgi. Primer sequences are as follows (F: forward, R: reverse; m: mouse; h: human): 5'-GTA CCT CCA CCA TGC CAA GT-3' (mhF2); 5'-CAC ACA GGA TGG CTT GAA GA-3' (hmR1); 5'-CTC ACC AAA GCC AGC ACA TA-3' (mhF3); 5'-TGG CTC ACC GCC TTG GCT-3' (mhR1); 5'-TTA ATC GGT CTT TCC GGT GA-3' (mR2); 5'-AAA TGC TTT CTC CGC TCT GA-3' (mhR3). We used hypoxantine-guanine phosphoribosyltransferase as an internal positive control as previously described (Carmeliet et al, 1999); the primer sequences were 5'-TTA TCA GAC TGA AGA GCT ACT GTA ATG ATC (HPRT-F1) and 5'-TTA CCA GTG TCA ATT ATA TCT TCA ACA ATC-3' (HPRT-R1). Primers were synthesized by Integrated DNA Technologies (Coralville, Iowa), and the optimal cycling conditions for their use determined as described in the *Taq*-Man PCR Reagents protocol. Nontumor human and mouse total RNA used as positive controls (mouse lung and ovary, and human brain) were obtained from Ambion (Austin, Texas). Five microliters of each RT reaction (sample), or of RNA samples that had not been reverse-transcribed (minus-RT control), were then amplified in triplicate in 96-well plates following the standard conditions for the *Taq*-Man PCR kit (PE Applied Biosystems) using an ABI 7700 System (PE Applied Biosystems). Three tumors were used for each data point, with consistent results, and thus the results shown are one representative example. The size of the PCR products was assessed by electrophoresis of 1/10 of the volume of the RT-PCR reactions on 4% NuSieve 3:1 agarose precast gels (FMC, Rockland, Maine) and comparison with several DNA ladders (PCR markers were from Novagen, Madison, Wisconsin; pGEM DNA marker was from Promega, Madison, Wisconsin; and 1-Kb ladder was from Gibco BRL, Rockville, Maryland).

ELISA for VEGF

To determine VEGF protein levels, tumors were resected and immediately frozen in liquid nitrogen. The tissues were homogenized in 1 ml of 50 mM Tris-HCl buffer pH 7.4 containing 0.25% Triton X-100, 0.5 M EDTA, 0.1% NP-40 and protease inhibitor cocktail (Completeprotease inhibitors; Roche Biochemicals, Indianapolis, Indiana). The entire procedure was performed with the tissue at 4° C. The total protein level in each sample was determined by the Standard Lowry Method (Bio-Rad DC protein assay; Bio-Rad, Hercules, California). Tissue extracts were diluted with 50 mM Tris-HCl to yield samples with the same protein concentration. Fifty microliters of each sample were used to determine VEGF levels. Mouse and human recombinant VEGF were obtained from R & D Systems (Minneapolis, Minnesota). Mouse and human levels of immunoreactive VEGF were quantified using separate Sandwich ELISAs specific to mouse and human VEGF, respectively (Quantikine Murine and Quantikine Human VEGF Immunoassay kits; R&D Systems), according to the manufacturer's recommended protocols.

In Vitro Cell Viability Assay

The effect of VEGF on tumor cell proliferation was assessed by MTT dye reduction assay (Mossamann and Young, 1983). PANC-1 cells were plated at the density of 1×10^3 cells/well in 96-well plates in 200 μl DMEM containing 10% FBS and 1% antibiotics. After 24 hours, the medium was changed to serum-free DMEM containing 5 ng/ml of recombinant (r) $VEGF_{121}$, or $VEGF_{165}$ (R & D Systems) with or without antihuman VEGF (Presta et al, 1997) or isotype-matched IgG1 as a control antibody with the concentrations of 800 ng/ml (Adamis et al, 1996). Anti-VEGF antibody or control antibody was added to the medium 2 hours before adding rVEGF protein and cells were grown for 24 hours. Medium was replenished and cells were grown for an additional 24 hours. After this period, cells were incubated for 1 hour in DMEM containing 0.42 mg/ml of MTT; the medium was then removed and the cells were lysed in dimethyl sulfoxide. The conversion of MTT to formazan by metabolically viable cells was monitored as a function of the optical density by a 96-well microtiter plate reader at 570 nm.

In Vivo Anti-VEGF Antibody Treatment

Four weeks after the tumor implantation, orthotopic or ectopic PANC-1 tumor–bearing mice were given murine antihuman VEGF neutralizing monoclonal antibody A.4.6.1 (a generous gift from Genentech, South San Francisco, California), 300 μg/mouse every 3 days ip (Presta et al, 1997; Yuan et al, 1996). As a control, the same amount of nonspecific murine IgG

was used. The treatments were continued for 4 weeks, followed by intravital microscopy analysis.

Statistics

Results are presented as mean ± SEM. Values of different groups were compared using a Mann-Whitney *U* test (StatView, Abacus, Berkeley, California). Significance was assumed for $p < 0.05$.

Acknowledgements

We thank Dr. Lance L. Munn for his helpful input on this study, Drs. Peigen Huang and Emmanuelle di Tomaso for histologic evaluation, and Ms. Sylvie Roberge for technical assistance.

References

Adamis A, Shima D, Tlentino M, Gragoudas E, Ferrara N, Folkman J, D'Amore P, and Miller J (1996). Inhibition of vascular endothelial growth factor prevents retina: Ischemia-associated iris neovascularization in a nonhuman primate. Arch Ophthalmol 114:66–71.

An Z, Wang X, Kubota T, Moossa AR, and Hoffman RM (1996). A clinical nude mouse metastatic model for highly malignant human pancreatic cancer. Anticancer Res 16:627–632.

Brunicardi FC, Stagner J, Bonner-Weir S, Wayland H, Kleinman R, Livingston E, Guth P, Menger M, McCuskey R, Intaglietta M, Charles A, Ashley S, Cheung A, Ipp E, Gilman S, Howard T, and Passaro E Jr (1996). Microcirculation of the islets of Langerhans. Long Beach Veterans Administration Regional Medical Education Center Symposium. Diabetes 45:385–392.

Bruns C, Harbison M, Kuniyasu H, Eue I, and Fidler I (1999). In vivo selection and characterization of metastatic variants from human pancreatic adenocarcinoma by using orthotopic implantation in nude mice. Neoplasia 1:50–62.

Carmeliet P, Dor Y, Herbert JM, Fukumura D, Brusselmans K, Dewerchin M, Neeman M, Bono F, Abramovitch R, Maxwell P, Koch CJ, Ratcliffe P, Moons L, Jain RK, Collen D, Keshert E, and Keshet E (1998). Role of HIF-1α in hypoxia-mediated apoptosis, cell proliferation and tumour angiogenesis. Nature 394:485–490.

Carmeliet P and Jain RK (2000). Angiogenesis in cancer and other diseases. Nature 407:249–257.

Carmeliet P, Ng YS, Nuyens D, Theilmeier G, Brusselmans K, Cornelissen I, Ehler E, Kakkar VV, Stalmans I, Mattot V, Perriard JC, Dewerchin M, Flameng W, Nagy A, Lupu F, Moons L, Collen D, D'Amore PA, and Shima DT (1999). Impaired myocardial angiogenesis and ischemic cardiomyopathy in mice lacking the vascular endothelial growth factor isoforms VEGF164 and VEGF188. Nat Med 5:495–502.

Dvorak HF, Nagy JA, Feng D, Brown LF, and Dvorak AM (1999). Vascular permeability factor/vascular endothelial growth factor and the significance of microvascular hyperpermeability in angiogenesis. Curr Top Microbiol Immunol 237:97–132.

Egami H, Tomioka T, Tempero M, Kay D, and Pour P (1991). Development of intrapancreatic transplantable model of pancreatic duct adenocarcinoma in Syrian golden hamsters. Am J Pathol 138:557–561.

Ellenrieder V, Adler G, and Gress T (1999). Invasion and metastasis in pancreatic cancer. Ann Oncol 10:46–50.

Ellis LM, Takahashi Y, Fenoglio CJ, Cleary KR, Bucana CD, and Evans DB (1998). Vessel counts and vascular endothelial growth factor expression in pancreatic adenocarcinoma. Eur J Cancer 34:337–340.

Ferrara N (1999). Role of vascular endothelial growth factor in the regulation of angiogenesis. Kidney Int 56:794–814.

Fidler IJ (1991). Orthotopic implantation of human colon carcinomas into nude mice provides a valuable model for the biology and therapy of metastasis. Cancer Metastasis Rev 10:229–243.

Fidler IJ, Wilmanns C, Staroselsky A, Radinsky R, Dong Z, and Fan D (1994). Modulation of tumor cell response to chemotherapy by the organ environment. Cancer Metastasis Rev 13:209–222.

Folkman J (2000). Tumor angiogenesis. In: Holand JF, Frei EI, Bast RCJ, Kufe DW, Pollock PE, and Weichselbauum RR, editors. Cancer Medicine, 5th ed. Ontario: B. C. Decker, Inc., 132–152.

Friess H, Yamanaka Y, Kobrin M, Do D, Buchler M, and Korc M (1995). Enhanced erbB-3 expression in human pancreatic cancer correlates with tumor progression. Clin Cancer Res 1:1413–1420.

Fujimoto K, Hosotani R, Wada M, Lee J, Koshiba T, Miyamoto Y, Tsuji S, Nakajima S, Doi R, and Imamura M (1998). Expression of two angiogenic factors, vascular endothelial growth factor and platelet-derived endothelial cell growth factor in human pancreatic cancer, and its relationship to angiogenesis. Eur J Cancer 34:1439–1447.

Fukumura D, Salehi HA, Witwer B, Tuma RF, Melder RJ, and Jain RK (1995). Tumor necrosis factor α-induced leukocyte adhesion in normal and tumor vessels: Effect of tumor type, transplantation site, and host strain. Cancer Res 55:4824–4829.

Fukumura D, Yuan F, Monsky WL, Chen Y, and Jain RK (1997). Effect of host microenvironment on the microcirculation of human colon adenocarcinoma. Am J Pathol 151:679–688.

Gohongi T, Fukumura D, Boucher Y, Yun CO, Soff GA, Compton C, Todoroki T, and Jain RK (1999). Tumor-host interactions in the gallbladder suppress distal angiogenesis and tumor growth: Involvement of transforming growth factor beta1. Nat Med 5:1203–1208.

Hanahan D (1985). Heritable formation of pancreatic beta-cell tumours in transgenic mice expressing recombinant insulin/simian virus 40 oncogenes. Nature 315:115–122.

Hawes R, Xiong Q, Waxman I, Chang K, Evans D, and Abbruzzese J (2000). A multispecialty approach to the diagnosis and management of pancreatic cancer. Am J Gastroenterol 95:17–31.

Hobbs SK, Monsky WL, Yuan F, Roberts G, Griffith L, Torchillin V, and Jain RK (1998). Regulation of transport pathways in tumor vessels: Role of tumor type and host microenvironment. Proc Natl Acad Sci USA 95:4607–4612.

Houck K, Ferrara N, Winer J, Cachianes G, Li B, and Leung D (1991). The vascular endothelial growth factor family: Identification of a fourth molecular species and characterization of alternative splicing of RNA. Mol Endocrinol 5:1806–1814.

Houck K, Leung D, Rowland A, Winer J, and Ferrara N (1992). Dual regulation of vascular endothelial growth factor bioavailability by genetic and proteolytic mechanisms. J Biol Chem 267:26031–26037.

Itakura J, Ishiwata T, Friess H, Fujii H, Matsumoto Y, Buchler M, and Korc M (1997). Enhanced expression of vascular endothelial growth factor in human pancreatic cancer correlates with local disease progression. Clin Cancer Res 3:1309–1316.

Itakura J, Ishiwata T, Shen B, Kornmann M, and Korc M (2000). Concomitant over-expression of vascular endothelial growth factor and its receptors in pancreatic cancer. Int J Cancer 85:27–34.

Izuishi K, Kato K, Ogura T, Kinoshita T, and Esumi H (2000). Remarkable tolerance of tumor cells to nutrient deprivation: Possible new biochemical target for cancer therapy. Cancer Res 60:6201–6207.

Jain RK (1997). The Eugene M. Landis Award Lecture: Delivery of molecular and cellular medicine to solid tumors. Microcirculation 4:1–23.

Jain RK (1998). The next frontier of molecular medicine: Delivery of therapeutics. Nat Med 4:655–657.

Jain RK and Munn LL (2000). Leaky vessels? Call Ang1! Nat Med 6:131–132.

Kitadai Y, Bucana CD, Ellis LM, Anzai H, Tahara E, and Fidler IJ (1995). In situ mRNA hybridization technique for analysis of metastasis-related genes in human colon carcinoma cells. Am J Pathol 147:1238–1247.

Leunig M, Yuan F, Menger MD, Boucher Y, Goetz AE, Messmer K, and Jain RK (1992). Angiogenesis, microvascular architecture, microhemodynamics, and interstitial fluid pressure during early growth of human adenocarcinoma LS174T in SCID mice. Cancer Res 52:6553–6560.

Lieber M, Mazzetta J, Nelson-Rees W, Kaplan M, and Todaro G (1975). Establishment of a continuous tumor-cell line (panc-1) from a human carcinoma of the exocrine pancreas. Int J Cancer 15:741–747.

McCuskey R (1997). In vivo microscopy of the exocrine pancreas. Microsc Res Tech 37:450–455.

Melder RJ, Koenig GC, Witwer BP, Safabakhsh N, Munn LL, and Jain RK (1996). During angiogenesis, vascular endothelial growth factor and basic fibroblast growth factor regulate natural killer cell adhesion to tumor endothelium. Nat Med 2:992–997.

Monsky WL, Fukumura D, Gohongi T, Ancukiewcz M, Weich HA, Torchilin VP, Yuan F, and Jain RK (1999). Augmentation of transvascular transport of macromolecules and nanoparticles in tumors using vascular endothelial growth factor. Cancer Res 59:4129–4135.

Mossamann PB and Young LL (1983). Rapid colorimetric assay for cellular growth and survival: Application to proliferation and cytotoxic assay. J Immunol Methods 65:49–53.

Parker S, Tong T, Bolden S, and Wingo P (1997). Cancer statistics, 1997. CA Cancer J Clin 47:5–27.

Pluen A, Bocher Y, Ramanujan S, McKee TD, Gohongi T, di Tomaso E, Brown EB, Izumi Y, Campbell RB, Berk DA, and Jain RK (2001). Role of tumor-host interactions in interstitial diffusion of macromolecules: Cranial vs subcutaneous tumors. Proc Natl Acad Sci USA 98:4628–4633.

Poltorak Z, Cohen T, Sivan R, Kandelis Y, Spira G, Vlodavsky I, Keshet E, and Neufeld G (1997). VEGF145, a secreted vascular endothelial growth factor isoform that binds to extracellular matrix. J Biol Chem 272:7151–7158.

Presta L, Chen H, O'Connor S, Chisholm V, Meng Y, Krummen L, Winkler M, and Ferrara N (1997). Humanization of an anti-vascular endothelial growth factor monoclonal antibldy for the therapy of solid tumors and other disorders. Cancer Res 57:4593–4599.

Ruoslahti E and Rajotte D (2000). An address system in the vasculature of normal tissue and tumors. Annu Rev Immunol 18:813–827.

Schmidt J, Ryschich E, Maksan S, Werner J, Gebhard M, Herfarth C, and Klar E (1999). Reduced basal and stimulated leukocyte adherence in tumor endothelium of experimental pancreatic cancer. Int J Pancreatol 26:173–179.

Terris B, Scoazec J, Rubbia L, Bregeaud L, Pepper M, Ruszniewski P, Belghiti J, Flejou J, and Degott C (1998). Expression of vascular endothelial growth factor in digestive neuroendocrine tumours. Histopathology 32:133–138.

Tischer E, Mitchell R, Hartman T, Silva M, Gospodarowicz D, Fiddes J, and Abraham J (1991). The human gene for vascular endothelial growth factor: Multiple protein forms are encoded through alternative exon splicing. J Biol Chem 266:11947–11954.

Tsuzuki Y, Fukumura D, Oosthuyse B, Koike C, Carmeliet P, and Jain RK (2000). Vascular endothelial growth factor (VEGF) modulation by targeting hypoxia inducible factor-1α $\rightarrow$ Hypoxia response element $\rightarrow$ VEGF cascade differentially regulates vascular response and growth rate in tumors. Cancer Res 60:6248–6252.

Von Marschall Z, Cramer T, Hocker M, Burde R, Plath T, Schirner M, Heidenreich R, Breier G, Riecken E, Wiedenmann B, and Rosewicz S (2000). De novo expression of vascular endothelial growth factor in human pancreatic cancer: Evidence for an autocrine mitogenic loop. Gastroenterology 119:1358–1372.

Wayland H (1997). Microcirculation in pancreatic function. Microsc Res Tech 37:418–433.

Yuan F, Chen Y, Dellian M, Safabakhsh N, Ferrara N, and Jain RK (1996). Time-dependent vascular regression and permeability changes in established human tumor xenografts induced by an anti-vascular endothelial growth factor/vascular permeability factor antibody. Proc Natl Acad Sci USA 93: 14765–14770.

Yuan F, Leunig M, Berk DA, and Jain RK (1993). Microvascular permeability of albumin, vascular surface area, and vascular volume measured in human adenocarcinoma LS174T using dorsal chamber in SCID mice. Microvasc Res 45:269–289.